

PFA Oriented ECAL Optimization for the CEPC

H.Zhao^{a,b,c} M.Ruan^{a,1} C.Fu^a D.Yu^{d,a} B.Ma^a Z.Wang^a T.Hu^a

^a*Institute of High Energy Physics, Chinese Academy of Sciences
Beijing 100049, China*

^b*CAS Center for Excellence in Particle Physics*

^c*Collaborative Innovation Center for Particles and Interactions*

^d*Laboratoire Leprince-Ringuet, Ecole Polytechnique
Palaiseau, France*

E-mail: manqi.ruan@ihep.ac.cn

ABSTRACT: The design and optimization of the Electromagnetic Calorimeter (ECAL) are crucial for the Circular Electron Positron Collider (CEPC) project, a proposed future Higgs/Z factory. Following the reference design of the International Large Detector (ILD), a set of silicon-tungsten sampling ECAL geometries are implemented into the Geant4 simulation, whose performance is then scanned using Arbor algorithm. At single particle level, the photon energy response at different ECAL longitudinal structures is analyzed. At bi-particle sample, the separation performance with different ECAL transverse cell sizes is investigated and parametrized. The overall performance is characterized by a set of physics benchmarks, including $\nu\nu H$ events where Higgs boson decays into a pair of photons (EM objects) or gluons (jets) and $Z \rightarrow \tau^+\tau^-$ events. Based on these results, we proposed an optimized ECAL geometry for the CEPC project.

KEYWORDS: Calorimeter methods, Simulation methods and programs, Detector modelling and simulations I

¹Corresponding author.

Contents

1	Introduction	1
2	Geometries and Simulation Tools	2
3	Arbor Reconstruction of Photon	3
3.1	Reconstruction of single photon by Arbor	3
3.2	Di-photon separation by Arbor	3
4	Optimization on ECAL Longitudinal Structure	4
4.1	Total Absorber Thickness	4
4.2	Sensitive Thickness and Number of Layer	7
5	Optimization on ECAL Cell Size	9
6	Conclusion	10

1 Introduction

After the Higgs discovery [1, 2], precise measurements of the Higgs boson properties and the Standard Model (SM) are vital for the particle physics. Proposed by the Chinese high energy physics community, the CEPC [3] project is expected to boost the precision of Higgs properties and Electroweak measurements by orders of magnitudes. The physics program at CEPC requires a detector that can reconstruct a full spectrum of physics objects with great efficiency and precision. The Particle Flow Algorithm (PFA) [4] oriented detector design is therefore of strong physics interests, as it reconstructs every final state particle, providing remarkable efficiency in physics object reconstruction.

Segmented in both longitudinal and transverse directions, a high granular ECAL is crucial for the PFA as it provides the necessary separations between the shower clusters induced by different final state particles. On the other hand, such PFA oriented ECAL is usually expensive and consumes lots of power. The ECAL optimization is crucial to control the construction cost, the power consumption, and to maintain the core physics performance.

Reducing the number of readout channels means either reducing the number of longitudinal layers or increasing the transverse cell size. The former will mainly affect the photon energy resolution and lepton/particle identification [5]. The latter will cause a degrading in the position and angular measurement for the neutral particles, especially the photons. More importantly, increasing the transverse cell size will significantly limit the shower separation performance, which is of key importance for the PFA.

In this manuscript, we will focus on the optimization study of these local ECAL geometry parameters: total absorber thickness, longitudinal layer number, silicon sensor thickness, and

transverse cell size. Using Arbor [6] algorithm and starting from the CEPC benchmark detectors, we explored the performance dependence on these parameters at a set of benchmark performances. For the longitudinal structure, the parameters are compared through the intrinsic photon energy resolution, which is characterized by single photon energy resolution and the mass resolution of Higgs boson via di-photons final states. For the transverse cell size, the EM-shower separation capability is chosen as the benchmark, and the impact is also evaluated on the Higgs boson mass resolution with jet final states ($\nu\nu H \rightarrow \nu\nu gluon$).

This manuscript is organized as follows. Section 2 gives a brief introduction to the simulated geometries and software tools. Section 3 is devoted to the photon reconstruction and EM-shower separation performances. The results of optimization studies are reported in Section 4, including the longitudinal parameters scan and the transverse cell size scan. The conclusion is summarized in Section 6.

2 Geometries and Simulation Tools

The International Large Detector (ILD) [7] design is one of the best understood PFA oriented detector design for the future electron positron colliders, providing an excellent reference for the CEPC detector design. A conceptual benchmark detector geometry for CEPC Pre-CDR study, CEPC_v1 [8], was developed and implemented into the Geant4 [9] simulation. Similar to ILD, CEPC_v1 uses sampling structure ECAL that is composed of silicon sensors and tungsten absorber plates. The total absorber thickness is 84 mm, divided into 30 longitudinal layers. Each layer consists of a 500-micrometer silicon sensor layer. Transversely, the sensor plate is segmented into 5 mm square readout cells.



Figure 1. A simulated simplified ECAL structure.

The CEPC_v1 simulation models the cracks between ECAL modules, staves, and the dead zone between ECAL barrel and endcaps. These defects may significantly impact the physics performance. Meanwhile, before reaching ECAL, the photons could also interact with the materials before ECAL. To evaluate the impact of geometry defects and the materials before ECAL, a simplified, defect-free ECAL geometry has also been implemented. This simplified ECAL geometry consists of a cylindrical barrel and two endcaps, forming a closed cylinder. It abstracts a few parameters to describe both global structure and local ECAL structure. The global parameters include the inner radius, the barrel length, the endcap outer radius, and the opening angles at the endcap. For the local structure, the longitudinal layout is described by the number of layers and the material

compositions/thickness in each layer, while the transverse structure is described by the cell size in two orthogonal directions.

In this manuscript, we focus on the local parameters optimization and thus the global parameters are determined according to CEPC v_1. The baseline geometry at the CEPC v_1 was used as the start point for local parameters optimization. For simplicity, all the tungsten plates have the same thickness. The simplified ECAL is also divided into 30 layers, each consist of 2.8 mm tungsten, 0.5 mm silicon, and 2 mm PCB layers. The transverse cell size is 5 mm by 5 mm.

3 Arbor Reconstruction of Photon

PFA attempts to identify and reconstruct all the final-state particles in the most suited sub-detector systems. Explicitly, PFA reconstructs charged particles in the tracking system, photons in the ECAL and neutral hadrons in the whole calorimeter. Arbor [6], the core reconstruction algorithm of CEPC, has been used for these optimization studies in this paper. The PFA performance can be characterized by energy response at single particle sample and separation performance at bi-particle sample. We will discuss both of them with photons.

3.1 Reconstruction of single photon by Arbor

A particle shower is usually composed of a compact core and a loose halo. The core usually develops along the direction of the initial particle and contains most of the energy. The halo usually consists of many low energy clusters and isolated hits induced by secondary particles and contains minority energy of the shower. As for EM-showers, higher hits and energy collection efficiency usually leads to a better energy resolution. However, the over merging between the core and the nearby clusters could cause the confusion between showers. Therefore, the overall performance relies on the balance of these two effects.

To characterize the reconstruction performance of single photon, we studied the photon finding efficiency and the photon shower energy collection efficiency at different energies. The photon finding efficiency is defined as the probability that Arbor could find at least one cluster once the photon is incident to the ECAL fiducial region. The energy collection efficiency is defined as the ratio between energies in the clusters and in all the calorimeter hits.

With simplified ECAL geometry, The finding efficiency reaches 100% for photons with energy larger than 500 MeV. The finding efficiency decreases to 85% once the photon energy is reduced to 100 MeV. The energy collection efficiency is better than 99% when the photon energy ranges from 1 GeV to 175 GeV. When the photon energy is less than 1 GeV, the energy collection efficiency degrades, i.e., the average energy collection efficiency decreases to 75% for 100 MeV photons. Since the simplified ECAL has no material before the calorimeter, it maintains high efficiencies even for low energy photons.

3.2 Di-photon separation by Arbor

The shower separation ability is crucial for the PFA reconstruction. It is highly appreciated in the jet energy resolution, the π_0 reconstruction, and the τ reconstruction. We characterized the EM-shower separation performance by the reconstruction efficiency of nearby di-photon events.

The di-photon sample simulates two parallel photons vertically incident into ECAL. According to the photon energy distribution at CEPC, the photon energy is set to 5 GeV.

To quantify the separation performance, we defined the reconstruction efficiency as the probability to successfully reconstruct two photons with anticipated energy. An event would be marked as successfully reconstructed if both the reconstructed photon has more than $1/3$ and less than $2/3$ of all the deposit energy. Figure 2 shows a successfully reconstructed di-photon event.

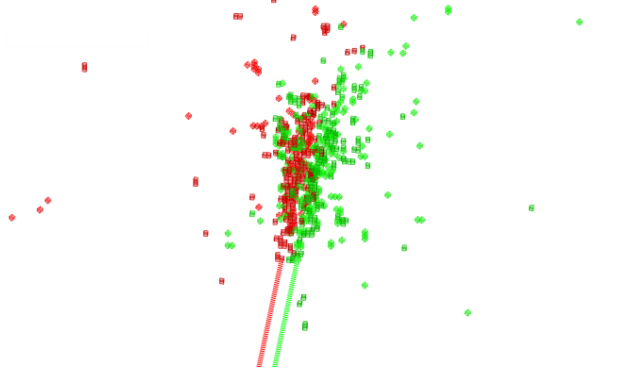


Figure 2. A reconstructed di-photon event with 1mm cell size ECAL. Each photon has an energy of 5 GeV, and the distance between them is 4 mm.

This probability depends mainly on the separation distance and the ECAL cell size, as shown in Figure 3. The distance between expected impact points of the two photons is scanned from 1 to 80 mm, with the cell size ranges from 1 mm by 1 mm to 20 mm by 20 mm. The parameters of Arbor are adjusted at different cell sizes. At large distance, for any cell size, the separation efficiency converges to ~ 1 since these photon showers become dis-entangled. At very short distance, the showers overlaps and the reconstruction efficiency drops steeply. Once the two photons are shot at exactly the same position, Arbor cannot distinguish the overlapped showers and the reconstruction efficiency vanishes. The unsmooth patterns in Figure 3 are induced by the finite cell size.

The critical separation distance is then defined as the distance at which 50% of the events are successfully reconstructed. When the cell size is larger than $4 \text{ mm} \times 4 \text{ mm}$ and smaller than the Moliere radius, the critical separation distance is roughly twice of the cell size, see Figure 4.

4 Optimization on ECAL Longitudinal Structure

In CEPC v_1 geometry, the ECAL is divided into 30 layers, and each layer contains tungsten as absorber layer, silicon as sensor layer and PCB as electronics/service layer. The longitudinal structure is essential for the intrinsic photon energy resolution, .e.g. the total absorber thickness will decide the energy leakage ratio of EM-showers and the thickness of silicon sensor will decide the sampling ratio. In this section, we will discuss these effects and propose an optimized longitudinal structure.

4.1 Total Absorber Thickness

The total absorber thickness of ECAL can be determined by the requirement on the longitudinal leakage of the most energetic electromagnetic showers. Giving the fact that CEPC would be

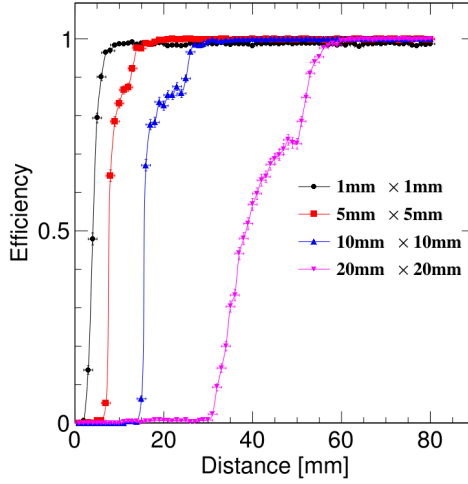


Figure 3. Reconstruction efficiency of di-photon samples at different cell size. The distance of the photons is scanned from 1 to 80 mm.

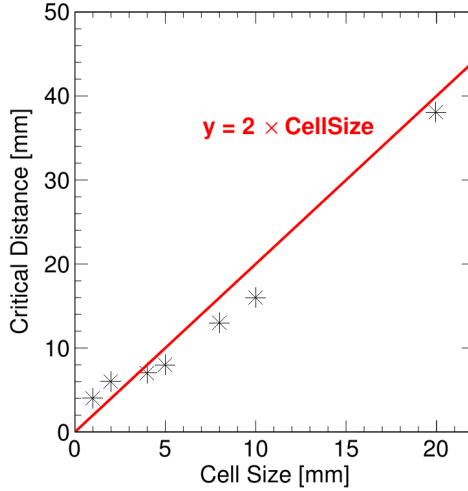


Figure 4. The critical separation distance at different cell size.

operating at 91-240 GeV center of mass energy, the most energetic electromagnetic particles are generated from the Bhabha events, the ISR return events and the Higgs events with Higgs bosons decay into photons. The final state photons of $H \rightarrow \gamma\gamma$ decay can be as high as 100 GeV at CEPC Higgs runs. And the final state electrons of Bhabha events could reach half of the collision energy. Figure 5 shows the longitudinal energy distribution for 120 GeV photons at a thickened ECAL. 98.6% energy of the 120 GeV photon shower deposits at first 30 layers, each has 2.8 mm thick tungsten.

To optimize the total tungsten thickness, we reconstructed the $\nu\nu H, H \rightarrow \gamma\gamma$ events and compared the Higgs mass resolution with different absorber thickness. At the default setting, a mass resolution of 1.6% has been achieved, see the left plot of Figure 6. Using thinner absorber, the energy leakage would impact the reconstructed photon energy resolution. While at thicker

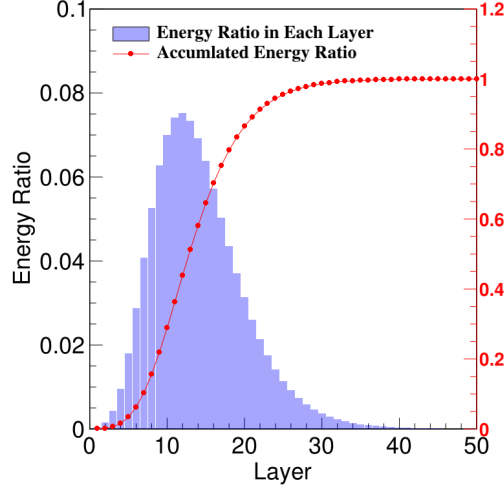


Figure 5. Ratio of 120 GeV photon shower energy deposited in each layer of SiW ECAL (with 50 layers, 2.8 mm tungsten, 0.5 mm silicon and 2mm PCB in each layer), and the integrated energy before each layer.

absorber, the resolution is mainly limited by the sampling ratio. A scan shows that the best Higgs mass resolution is achieved with the default tungsten thickness of 84 mm, see the right plot of Figure 6.

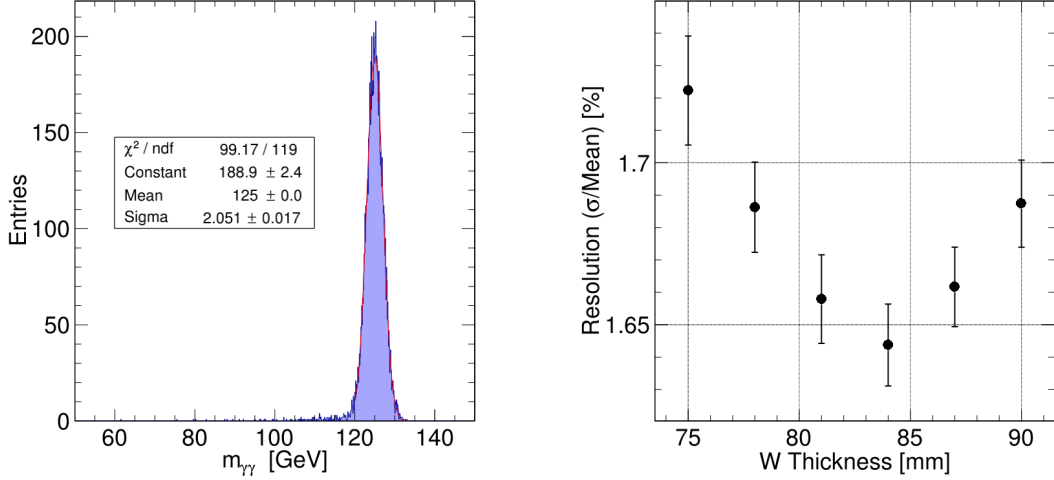


Figure 6. Higgs mass reconstructed from $\nu\nu\text{Higgs} \rightarrow \gamma\gamma$ events with 84 mm total tungsten thickness (left) and the resolution (σ/Mean) of reconstructed Higgs mass at different tungsten thickness (right).

Similar analysis has also been operated at CEPC_v1 geometry, where the geometry inhomogeneities, especially the cracks between ECAL modules and staves, make an significant impact on the accuracy. A geometry based correction is mandatory to control those effects. After a careful photon energy re-calibration, the degrading induced by these geometry effects can be controlled to better than 20%, or say, a Higgs mass resolution better than 2% can be achieved with CEPC_v1 geometry [10].

4.2 Sensitive Thickness and Number of Layer

The single photon energy resolution of simplified, 30-layer ECAL is displayed as the black curve in Figure 7, which is consistent with the test beam result of ILD ECAL prototype [11]. This set up then serves as a reference for the layer number optimization.

Reducing the number of layers means fewer read-out channels, which leads to lower construction cost and power consumption. Keeping the total absorber thickness at the optimized value of 84 mm, reducing the readout layer numbers and maintaining the local sensor thickness, the ECAL energy resolution degrades as the sensor-absorber ratio decreases. Figure 7 shows the impact on energy resolution if the number of layers is reduced to 25 and 20. Compared with 30 layers option, the energy resolution degrades by 11% at 25 layers and 27% at 20 layers.

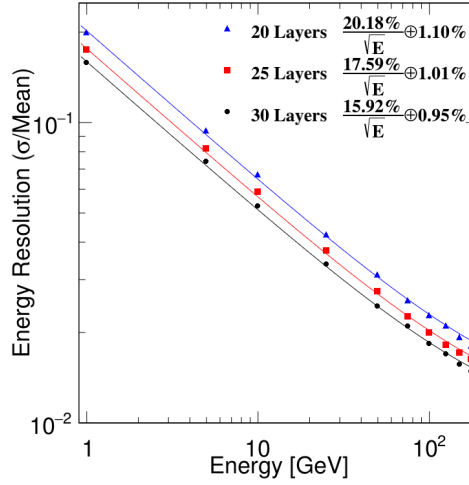


Figure 7. Impact on photon energy resolution when reducing the number of layer from 30 to 25 and 20, while the total thickness of absorber and the thickness of sensitive layer maintain the same.

The degrading of photon energy resolution by reducing the number of channels could be compensated by using thicker silicon sensor. We studied the energy resolution of ECAL at 20 layers with 1.5 mm thick silicon wafer and 25 layers with 1 mm thick wafer. These two options can achieve the same level energy resolution with 30 layers with 0.5 mm thick wafer option, as shown in Figure 8.

This result is confirmed at physics event with jet final states at CEPC_v1 geometry. Using $\nu\nu H, Higgs \rightarrow gluons$ events as the benchmark, the PFA performance is characterized by the Higgs boson mass resolution. A standard selection has been designed to veto events with energetic and visible ISR photon, events with significant neutrinos generated in gluon fragmentation, and events with jets aiming at beam pipe. This event selection has an overall efficiency of 65%. Figure 9 shows the distribution of reconstructed Higgs mass at 30 layers, 0.5 mm silicon ECAL after this event selection, where a mass resolution of 3.73% is observed. The mass resolutions with other longitudinal structures are shown in Table 1. Marginally difference has been observed in these different configuration. In considering possible systematic uncertainties from Arbor parameter optimization at different geometry, we consider these results consistent with the single photon results.

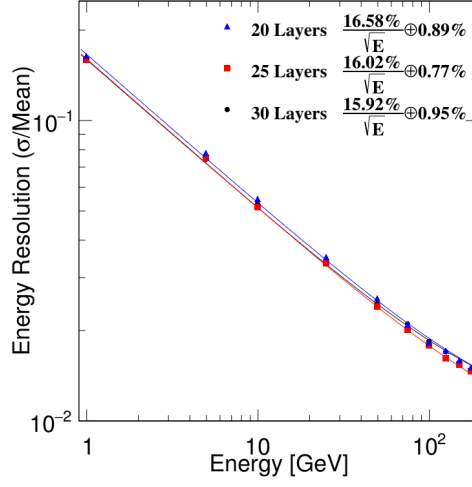


Figure 8. Energy resolution with less layers and thicker silicon wafer (20 layers with 1.5 mm silicon wafer and 25 layers with 1 mm silicon wafer), compared to 30 layers and 0.5 mm thick silicon wafer.

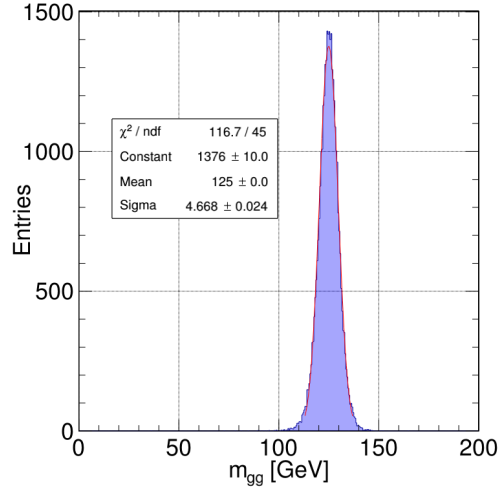


Figure 9. Higgs mass reconstructed from $\nu\nu H, Higgs \rightarrow glouns$ events with 30 layers, 0.5 mm silicon ECAL.

Table 1. Resolution of reconstructed Higgs mass through $\nu\nu H, Higgs \rightarrow glouns$ events using different longitudinal structures at CEPC_v1 geometry.

Layer number	Silicon sensor thickness	Higgs mass resolution (Statistic error only)
30	0.5 mm	$3.74 \pm 0.02 \%$
25	1 mm	$3.71 \pm 0.02 \%$
20	1.5 mm	$3.78 \pm 0.02 \%$

5 Optimization on ECAL Cell Size

In Section 3.2, we discussed the EM-shower separation ability at different ECAL cell size and characterize it with the critical separation distance. The impact of separation performance on physics events is evaluated at $Z \rightarrow \tau^+\tau^-$ events, for the following reasons. First of all, the reconstruction of physics events with τ final states leads to rich physics program and is of strong physics interest [12]. Secondly, the CEPC is a powerful Z factory and can produce hundreds of millions of $Z \rightarrow \tau^+\tau^-$ events. Thirdly, energetic π_0 s are generated in τ decay, which then decay into very closed photons. The successful reconstruction of the photons generated in τ decay therefore makes a clear physics requirement for the separation performance.

We calculate the impact position between photon to its closest neighbor(except for neutrino and muon) of the $Z \rightarrow \tau^+\tau^-$ events, as shown in Figure 10. We derive the percentage of photons whose distance to its closest neighbor is smaller than the critical separation distance with different ECAL cell size. As shown in Table 2, with the ECAL cell size is at 10 mm, the overlapping chance is 1.7% only. However, once the ECAL cell size increases to 20 mm, this overlapping chance rapidly increases by one order of magnitude.

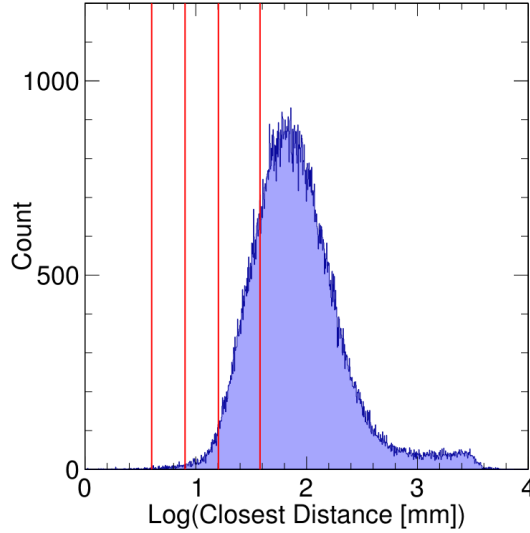


Figure 10. The distribution of the distance between photon and its closest neighbor, from $Z \rightarrow \tau^+\tau^-$ events at 91.2 GeV. The red line from left to right represents the critical separation distance when cell side length equals 1mm, 5mm, 10mm, 20mm.

Table 2. Percentages of photons that would be polluted by neighbor particles

Cell Size	Critical Separation Distance with Arbor	Percentage of $Z \rightarrow \tau^+\tau^-$
1 mm	4 mm	0.07%
5 mm	8 mm	0.30%
10 mm	16 mm	1.70%
20 mm	38 mm	19.63%

The reduced separation power also leads to a degraded Boson Mass Resolution. Characterized by the Higgs mass resolution at $\nu\nu H, Higgs \rightarrow gluons$ events, we compared the reconstructed Higgs mass resolution at 5 mm/10 mm/20 mm ECAL transverse cell size, as shown in Table 3. Within the statistic error, the Higgs mass resolution maintains at the same level if the transverse cell size is enlarged from 5 mm to 10 mm. When the cell size is further enlarged to 20 mm, a $\sim 5\%$ relative degrading is found. Based on this observation, we recommend the ECAL cell size should be equal or smaller to 10 mm.

Table 3. Resolution of reconstructed Higgs mass through $\nu\nu H, Higgs \rightarrow gluons$ events with different cell size at CEPC_v1 geometry.

Silicon sensor cell size	Higgs mass resolution (Statistic error only)
5 mm	$3.74 \pm 0.02\%$
10 mm	$3.75 \pm 0.02\%$
20 mm	$3.93 \pm 0.02\%$

6 Conclusion

The ECAL optimization is crucial for the CEPC detector design. Starting from the benchmark detector geometry at CEPC Pre-CDR study (CEPC_v1), we explored the physics performances at different ECAL geometries using Geant4 simulation and Arbor reconstruction. Based on the study results, we recommended a set of optimized ECAL geometry parameters.

The local ECAL geometry is determined by the longitudinal structure and the transverse cell sizes. In the original design at CEPC_v1 geometry, the ECAL has a total absorber thickness of 84 mm, divided into 30 longitudinal layers. Each longitudinal layer consists of one 500-micrometer silicon sensor layer, which is segmented into 5 mm readout cells (square shape). In this manuscript, we focused on these local ECAL geometry parameters: total absorber thickness, longitudinal layer number, silicon sensor thickness, and transverse cell size.

The longitudinal structure is essential for the intrinsic photon energy resolution, which is characterized by single photon energy resolution and the mass resolution of Higgs boson via di-photon final states. Using a simplified, defect-free ECAL geometry, we found that the single photon energy resolution reaches $15.92\%/\sqrt{E} \oplus 0.95\%$ (Figure 7), agrees with the CALICE test beam result [11]. A relative mass resolution of 1.64% is achieved for the Higgs mass measured from di photon final states channel, about 20% better than the result at CEPC v_1 geometry. Using $Higgs \rightarrow \gamma\gamma$ as the benchmark, we scanned the tungsten absorber thickness. Our study shows that 84mm total tungsten thickness is optimized for this benchmark measurement.

We also scanned the photon energy resolution at different numbers of longitudinal layers. Not surprisingly, reduced number of layers leads to worse performance. However, thicker silicon sensor layers could be used to compensate this degrading. Comparing the original design (30 longitudinal layers, each equipped with 500 μm thick silicon sensor layer) and the optimized design (25 longitudinal layers and 1 mm thick silicon layer), we observed the same level performance at single photon samples. The layer number could be further reduced to 20 layers, if thicker silicon

sensor (1.5 mm) could be adopted. This conclusion is cross-checked, and consistent with the analysis at physics benchmark of $\nu\nu H, Higgs \rightarrow gluons$ events.

The transverse cell size of ECAL dominant the shower separation performance, which is fundamental for the PFA performance. Using di-photon samples, we found that Arbor could efficiently separate particles as far as their impact position is distanced larger than twice the cell size (for cell size larger than $4\text{ mm} \times 4\text{ mm}$ and smaller than the Moliere radius). We studied the chances of photon overlapped with other particle showers at the $Z \rightarrow \tau^+\tau^-$ samples at 91.2 GeV center of mass energy. Our analysis shows that the photon overlapping chance maintains at a low level for cell size smaller than 10 mm (roughly 2%); however, increasing the cell size from 10 mm to 20 mm, the overlapping chance will be bowled up by one order of magnitudes. Meanwhile, at $\nu\nu H, Higgs \rightarrow gluons$ events sample, we observed a mass resolution of 3.74%/3.75%/3.93%, corresponding to 5 mm/10 mm/20 mm ECAL transverse cell size. Therefore, considering the physics requirements of the precise EW measurements, we recommend the cell size to be 10 mm or smaller.

The recommended ECAL geometry parameter is therefore summarized in Table 4. This set up fulfills the physics requirement for CEPC Higgs and EW measurements. Giving similar collision environments and physics objective, we believe this set up is also a reasonable starting point for the ECAL optimization for other electron positron Higgs/Z factories.

Table 4. Optimized ECAL local geometry parameters.

Layer number	25
Silicon wafer thickness	1 mm
Tungsten plate thickness	3.36 mm
Transverse cell size	5 - 10 mm

Acknowledgments

The author thanks Gang Li and Xin Mo for the physics event generator files. We appreciate Vincent Boudry, Vladislav Balagura and Henri Videau, at LLR, Ecole polytechnique, for their insights to high granularity calorimeter and discussions. This study is supported by National Key Program for S&T Research and Development (Grant No.: 2016YFA0400400), National Natural Science Foundation of China (No.: 11675202 and No.: 11675196), and the CAS Hundred Talent Program (Y3515540U1)

References

- [1] The ATLAS Collaboration, G. Aad et al., *Observation of a new particle in the search for the Standard Model Higgs boson with the ATLAS detector at the LHC*, *Phys. Lett. B* **716**(2012) 1-29, arXiv:1207.7214 [hep-ex].
- [2] The CMS Collaboration, S. Chatrchyan et al., *Observation of a new boson at a mass of 125 GeV with the CMS experiment at the LHC*, *Phys. Lett. B* **716**(2012) 30-61, arXiv:1207.7235 [hep-ex].
- [3] The CEPC-SPPC Study Group, *CEPC-SPPC Preliminary Conceptual Design Report*

- [4] M. Thomson, *Particle Flow Calorimetry and the PandoraPFA Algorithm*, *Nucl.Instrum.Meth* **A611**(2009) 25,40. arxiv:0907.3577[physics.ins-det]
- [5] D.Yu et al., *Lepton identification at particle flow oriented detector for the future $e+e-$ Higgs factories*, arXiv:1701.07542 [physics.ins-det]
- [6] M. Ruan and H. Videau, *Arbor, a new approach of the Particle Flow Algorithm*, arxiv:1403.4784 [physics.ins-det]
- [7] T. Behnke et al., *The International Linear Collider Technical Design Report -Volume 4: Detectors*(2013). arXiv:1306.6329 [physics.ins-det].
- [8] M.Ruan, *Status & Updates from CEPC Simulation-Detector optimization*, Presented on IAS, HK 2017
- [9] The GEANT4 Collaboration, S. Agostinelli et al., *GEANT4: A simulation toolkit*, *Nucl. Instrum. Meth. A* **506**(2003) 250-303.
- [10] M. Ruan, *Simulation, reconstruction and software at the CEPC*, presentation at CEPC workshop, April 2016, Beijing
- [11] Y. Sudo et al., *Development of a Highly Granular Silicon-Tungsten ECAL for the ILD*, *Nucl.Part.Phys.Proc.* 273-275 (2016)
- [12] Michel Davier et al., *The Physics of Hadronic Tau Decays*, *Review of Modern Physics* 78.4(2005):1043-1109.